Morphology and composition of hydroxyapatite coatings prepared by hydrothermal treatment on electrodeposited brushite coatings

YONG HAN, KEWEI XU
State-Key Laboratory for Mechanical Behaviour of Materials, Xi'an Jiaotong University, Xi'an 710049, People's Republic of China
E-mail: KWXU@XJTU01.XJTU.EDU.CN

JIAN LU
LASMIS (Mechanical Systems and Concurrent Engineering Laboratory), Universite de Technologie de Troyes, 12 rue Marie Curie, BP 2060, 10010 Troyes Cedex, France

Highly pure brushite ($CaHPO_4 \cdot 2H_2O$) coatings on porous Ti6Al4V substrates were prepared by electrodeposition from aqueous electrolytes. The influence of hydrothermal treatment parameters on brushite-to-hydroxyapatite conversion and the morphology and phase composition of hydroxyapatite (HAP) coatings was studied. It was found that the content, Ca/P atomic ratio, grain size and pore size of HAP in coatings increase with increasing hydrothermal treatment temperature, and that increasing the pH value can promote brushite-to-HAP conversion and reduce the grain size of HAP. Under optimal conditions, highly pure HAP coatings with needle-like crystals and non-stoichiometric form, which are similar to those of calcium phosphate in human bone, can be obtained.

1. Introduction

A typical formula for hydroxyapatite (HAP) is $Ca_{10-x}(HPO_4)_x(PO_4)_{6-x}(OH)_{2-x}$, where x ranges from 0–2, giving a Ca/P atomic ratio of between 1.67 and 1.33 [1]. Being a major constituent of bone, HAP not only has good biocompatibility [2], but also can possibly form strong chemical bonding with natural bone [3]. However HAP has some disadvantages, such as its brittleness, low tensile strength and fracture toughness. In fact, the brittleness is a serious obstacle to the application of HAP as load-bearing implants. HAP can, however, be effectively used as a coating on a metallic substrate. The coated implant will have the ductility of the underlying metal, as well as a bioactive surface. There are a number of additional benefits with this coating: faster adaptation of implant and surrounding tissue with reduced healing time [4], enhancement of bone formation [5], firmer implant bone attachment [6] and the reduction of metallic ion release [7].

Many techniques, such as physical vapor deposition, chemical vapor deposition, sol-gel, plasma spray and laser deposition, have been used to coat HAP on to metallic substrates. However, these techniques all present some drawbacks, as described elsewhere in detail [8, 9]. There is a possibility of decomposition of the HAP in coatings when the technique involves high-temperature processing steps. For instance, the plasma-sprayed HAP coating may contain tri- and tetracalcium phosphates, oxhydroxyapatite and amorphous calcium phosphates [10]. Ellies *et al.* [11] claimed that degradation of HAP in plasma-sprayed coating is severe if the starting powder is calcium-deficient HAP (d-HAP, $1.33 < Ca/P < 1.67$), and reported only 5% degradation in the coating deposited from stoichiometric HAP (s-HAP, $Ca/P = 1.67$) powder. The d-HAP is of greater biological interest than the s-HAP because the Ca/P ratio in bone apatite is between 1.67 and 1.5 [12]. Thus, it is necessary to explore the technique for coating HAP at relatively low temperature.

In 1956, Tiselius *et al.* [13] described a procedure in which crystalline brushite was prepared and then coated with HAP by boiling brushite in 1M NaOH (aqueous) for 1 h. In 1990, Redepenning *et al.* [14] improved the method to prepare brushite coating given by Tiselius *et al.* [13] by electrochemical deposition. Subsequent to this work, Shirkhanzadeh published several short papers demonstrating that similar results could be achieved using the same principles [15, 16], in which an electrochemically deposited coating was treated by steam rather than being boiled in NaOH solution. The microstructural characterization of the coating produced with this method is worth investigation for use in implants. In the present work, we prepared brushite coatings by electrochemical deposition and post-treated them by a hydrothermal process at relatively low temperature. The influence of hydrothermal treatment parameters on the morphology and composition of HAP in the coatings was studied in detail.

2. Experimental procedure

The sample substrate was Ti6Al4V plate. Its surface was mechanically ground and subsequently blasted with SiC grit. The electrolyte used to form the coating was produced by mixing 0.21M $Ca(NO_3)_2 \cdot 4H_2O$ and 0.125M $NH_4H_2PO_4$ solutions. The pH value of the electrolyte was adjusted to 4 by the addition of ammonia. Electrochemical deposition of the coating on Ti6Al4V was accomplished using a potentiostat. Two graphite rods were used as the anode and Ti6Al4V plate was used as the cathode. The coating process was carried out at 60 °C and 1.5 v for 1.5 h in a conventional electrolytic cell.

The electro-coated samples were mounted in an autoclave as shown in Fig. 1 to receive hydrothermal treatment for 8 h. The pH value of the water used for hydrothermal treatment was adjusted with ammonia. Table I lists the treatment state of samples, where the pH value of water used for treating samples in Group 1 is higher than 7 and kept constant.

The phase composition of coating was analyzed with X-ray diffractometry (XRD) and infrared spectroscopy (IR). The morphology of coating was observed by scanning electron microscopy (SEM). The Ca/P atomic ratio of crystals with various morphologies was tested by electron-dispersive analysis spectra (EDAX).

3. Results and discussion

3.1. The characterization of electrodeposited coatings

The electrochemically deposited coating is about 30 μm thick. Its structure is shown in Fig. 2. The coating consists of highly pure brushite ($CaHPO_4 \cdot 2H_2O$) with a plate-like crystallizing morphology. The Ca/P atom ratio in the plate-like crystals is 1.009, which is very close to that in bulk brushite. The parameters in the electrochemical deposition were adjusted, but the product in the coatings was always brushite, and only the porosity and crystal sizes changed. The following electrochemical reactions occur during the process [17]. First, water is reduced at the Ti6Al4V substrate to produce hydrogen gas and hydroxide ions, as shown in the following reaction:

$$2H_2O + 2e^- = H_2 + 2OH^- \quad (1)$$

Then, the hydroxide ions generated at the surface react with dihydrogen phosphate according to the equilibrium

$$OH^- + H_2PO_4^- \rightleftharpoons H_2O + HPO_4^{2-} \quad (2)$$

Finally, the produced HPO_4^{2-} ions combine with Ca^{2+} to form brushite according to the equilibrium shown below, and brushite deposits at the substrate surface

$$Ca^{2+} + HPO_4^{2-} + 2H_2O \rightleftharpoons CaHPO_4 \cdot 2H_2O \quad (3)$$

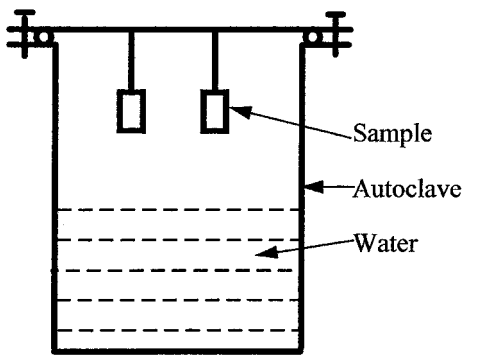

Figure 1 Schematic of apparatus for hydrothermal treatment.

3.2. The characterization of hydrothermally treated coatings

The XRD spectra of hydrothermally treated coatings are shown in Fig. 3, and the relative content of phases in the coatings is listed in Table II. When the pH value of water

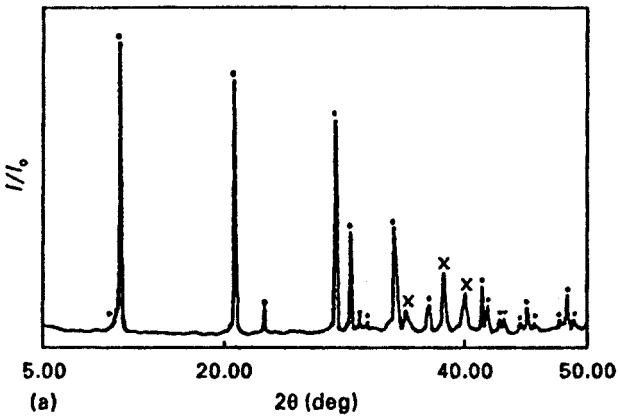

(a)

(b)

Figure 2 (a) XRD spectrum and (b) scanning electron micrograph of electrochemically deposited coating. (•) $CaHPO_4 \cdot 2H_2O$, (×)Ti.

TABLE I The hydrothermal treatment process on samples

	Group I				Group II			
Samples	A1	B1	C1	D1	E1	C2	D2	E2
pH value	> 7	> 7	> 7	> 7	> 7	7	7	7
Temperature°C	130	160	180	210	240	180	210	240

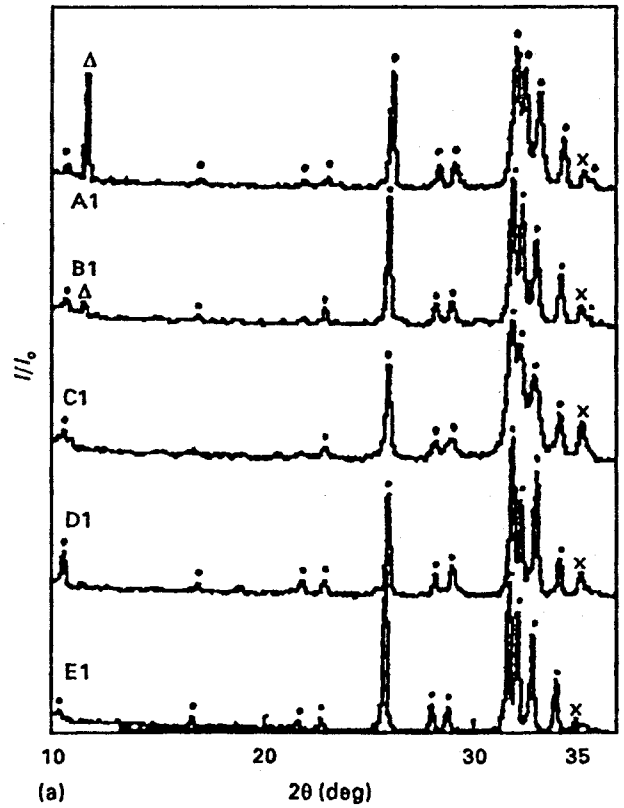

(a)

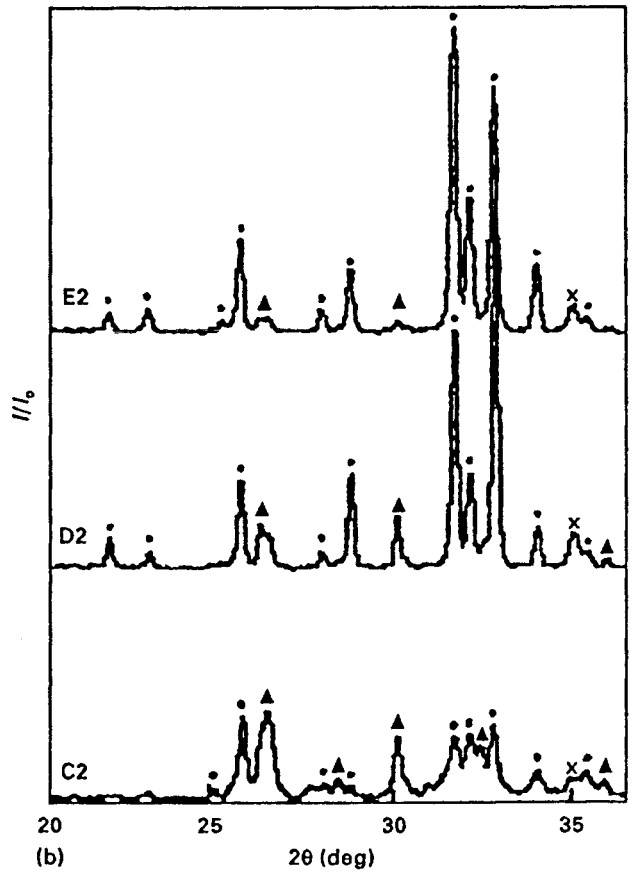

(b)

Figure 3 XRD spectra of hydrothermally treated samples (a) in Group I, (b) in Group II. (Δ)$CaHPO_4 \cdot 2H_2O$.(●)HAP, (×)Ti, (Δ)$CaHPO_4$.

TABLE II The phase analysis results of hydrothermally treated coatings

Samples	Phase composition		Ca/P ratio of HAP	Molecular formula of HAP
	Phases	Content (%)		
A1	HAP	59.3	1.56	$Ca_{9.36}(HPO_4)_{0.64}(PO_4)_{5.36}(OH)_{1.36}$
	$CaHPO_4 \cdot 2H_2O$	40.7		
B1	HAP	81.4	1.61	$Ca_{9.68}(HPO_4)_{0.34}(PO_4)_{5.66}(OH)_{1.66}$
	$CaHPO_4 \cdot 2H_2O$	18.6		
C1	HAP	100	1.63	$Ca_{9.78}(HPO_4)_{0.22}(PO_4)_{5.73}(OH)_{1.70}$
D1	HAP	100	1.67	$Ca_{10}(PO_4)_6(OH)_2$
E1	HAP	100	1.68	$Ca_{10}(PO_4)_6(OH)_2$
C2	HAP	43.5	1.62	$Ca_{9.72}(HPO_4)_{0.28}(PO_4)_{5.72}(OH)_{1.72}$
	$CaHPO_4$	56.5		
D2	HAP	76.8	1.67	$Ca_{10}(PO_4)_6(OH)_2$
	$CaHPO_4$	23.2		
E2	HAP	93	1.68	$Ca_{10}(PO_4)_6(OH)_2$
	$CaHPO_4$	7		

used for hydrothermal treatment is higher than 7, the content of HAP in coatings increases gradually with increasing treatment temperature. At above 180 °C, brushite in coating converts entirely to HAP and the coating consists of highly pure HAP. When the pH value of the water used for hydrothermal treatment is kept at 7, although the content of HAP in coating increases with increasing treatment temperature, there is still 7% $CaHPO_4$ in the coating. It is suggested that increasing pH value can promote brushite-to-HAP conversion.

The IR results of coatings C1 and E1 are shown in Fig. 4. Both coatings are composed of pure HAP. The peaks at 3571 and 633 cm^{-1} are due to OH^- groups. The 875 cm^{-1} peak is caused by HPO_4^{2-} groups. The bands at 1100–1033, 962, 602, 563 and 481 cm^{-1} are due to PO_4^{3-} groups. There is also a sharp peak at 1645 cm^{-1} and a broad band from 3600–2500 cm^{-1} indicative of absorbed water. Fig. 4 indicates that both coatings C1 and E1 contain OH^- and PO_4^{3-} groups, however, coating C1 also contains HPO_4^{2-} groups whereas E1 does not. Such results imply that HAP in coating C1 is calcium-deficient, and HAP in coating E1 is stoichometric. However, from Fig. 3, it is evident that the XRD pattern of d-HAP in coating C1 is substantially equivalent to that of s-HAP in coating E1, except for the peak width and intensity. This substantiates the idea that the structural deficiencies in d-HAP do not alter the basic crystalline arrangement.

Fig. 5 shows the morphology of various coatings (in Group 1) hydrothermally treated by water with pH > 7. In coatings A1 and B1, in addition to plate-like crystals, thin needle-like crystals (nanometer-size in diameter by micrometer-size in length) are found. Coatings C1, D1 and E1 are entirely made up of needle-like crystals. The sizes of the needle-like crystals and micropores between them increase with increasing treatment temperature. EDAX was used to measure the Ca/P atomic ratios of plate-like crystals in coatings A1 and B1, which were 0.998 and 1.009, respectively, and substantially equal to that of brushite. Based on such results and the phase composition of coatings A1 and B1, it is shown that the plate-like crystals in coatings A1 and B1 are composed of brushite, and that the residual brushite in the hydrothermally treated coatings still retains its original morphology. EDAX was also used to measure the Ca/P ratio of needle-like crystals in coatings A1, B1, C1, D1 and E1, which is 1.56, 1.61, 1.63, 1.67 and 1.68, respectively, corresponding to the Ca/P ratio of HAP. Thus, the phase of needle-like crystals in coatings A1, E1 is proved to be HAP. The porous coating C1 composed of d-HAP with a thin needle-like morphology, is expected to be of much greater biological interest. This is because the apatite in bone is in the form of thin needle-like crystals (5 20 nm diameter by 60 nm long) with a Ca/P molar ratio between 1.67 and 1.5 [18], and the porous HAP coatings can increase the rate of bone tissue ingrowth and enhance the mechanical fixation of porous-coated implants in a relatively short period of time after an operation [18].

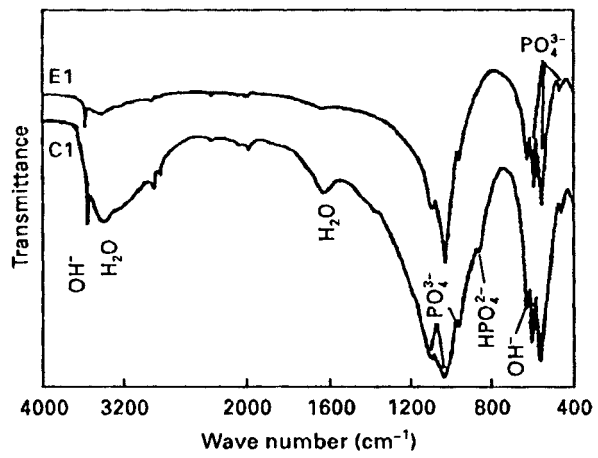

Figure 4 Infrared spectra of coatings C1 and E1.

Fig. 6 shows the morphology of various coatings (in Group H) hydrothermally treated by water with pH = 7. It is clear that there are twig-like crystals in coating C2 in addition to plate-like crystals, and that the diameter of the twig-like crystals and the size of the pores between them increase with increasing treatment temperature. The Ca/P ratio of plate-like crystals in coating C2, as indicated by EDAX, is 1.01. The Ca/P ratios of twig-like crystals in coatings C2, D2 and E2 as indicated by EDAX are 1.62, 1.67 and 1.68, respectively. Based on such results and the phase composition of coatings C2, D2 and E2 (with a biphasic $CaHPO_4$ + HAP structure), it is shown that the phase of twig-like crystals in coatings C2, D2 and E2 is HAP, and that of plate-like crystals is $CaHPO_4$. The specific molecular formula of HAP in various coatings,

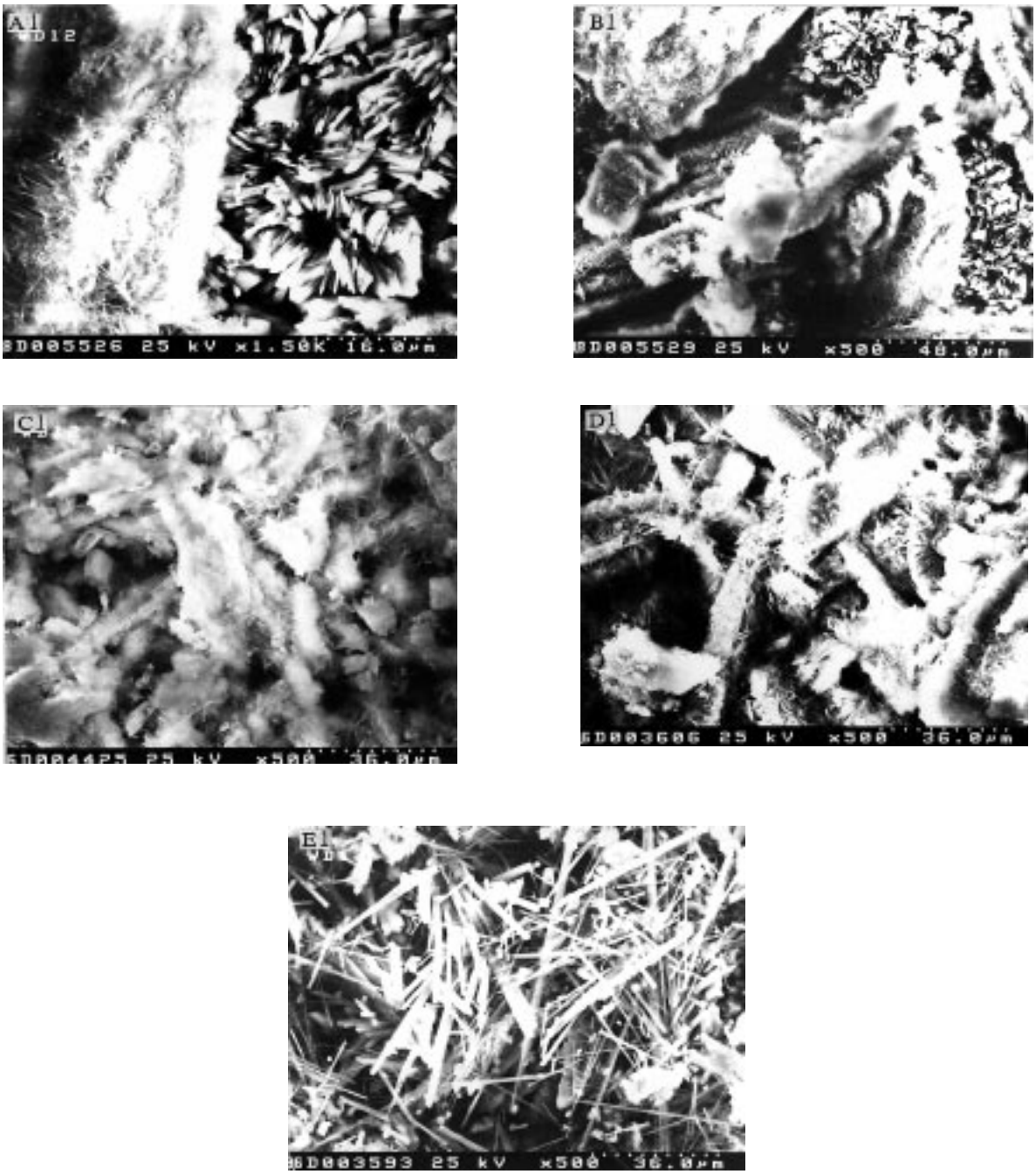

Figure 5 Scanning electron micrographs of coatings in Group 1. (a) A1, (b) B1, (c) C1, (d) D1, (e) E1.

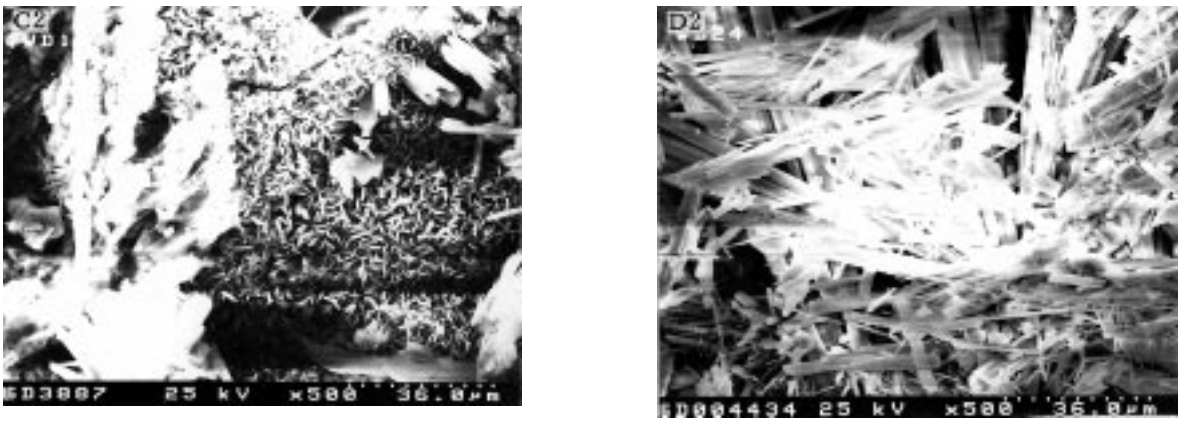

(a) (b)

Figure 6 Scanning electron micrographs of coatings in Group II. (a) C2, (b) D2, (c) E2.

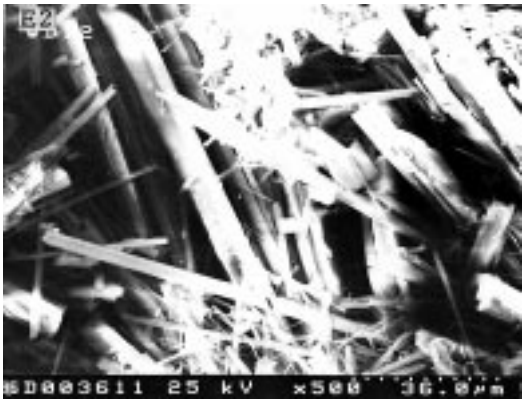

(c)

Figure 6 (Continued)

which was speculated in terms of the Ca/P atomic ratio, is given in Table II. This indicates that, with increasing treatment temperature, the Ca/P atomic ratio increases, and so HAP changes from the calcium-deficient form to the stoichiometric form. Comparing Figs 5 and 6 shows that at the same treatment temperature, with increasing pH value of the water used for hydrothermal treatment, the grain size of HAP in the coatings decreases remarkably, as does the size of pores between the grains. The morphology of HAP in the present coatings can be distinguished from that of Redepenning *et al*. [17] or Shirkhanzadeh [16], in which HAP appears to be plate-like.

The physical-chemical process during hydrothermal treatment can be analyzed as follows: when the water is vaporized, the following equilibrium is created [19]

$$H_2O \rightleftharpoons H^+ + OH^- \quad (4)$$

Thus, water vapor contains OH^- ions, and the content increases with increasing temperature. Then, OH^- ions in the vapor are expected to react with $CaHPO_4$ in the electrodeposited coating according to the following equilibrium

$$(10-x)CaHPO_4 + (12-x)OH^- \rightleftharpoons Ca_{10-x}(HPO_4)_x(PO_4)_{6-x}(OH)_{2-x} + (4-x)PO_4^{3-} + (10-x)H_2O \quad (5)$$

where x ranges from 0–2 and can be determined by the temperature and the concentration of OH^- ions. Thus, increasing the treatment temperature or pH value can promote the brushite-to-HAP conversion.

4. Conclusions

Highly pure brushite coatings on Ti6A14V substrates were prepared by electrodeposition from $Ca(NO_3)_2$ and $NH_4H_2PO_4$. The brushite could be converted to hydroxyapatite through hydrothermal treatment, and the structure of the coatings varied with hydrothermal treatment parameters as follows. At the same pH value, the content, Ca/P atomic ratio, grain size and pore size of HAP in the coatings increase with increasing treatment temperature. Increasing the pH value decreased the lowest temperature at which the brushite coating could be entirely converted to HAP coating. At the same treatment temperature, the sizes of grains and pores between the grains of HAP decreased with increasing pH value.

Under optimal conditions, highly pure HAP coatings with thin needle-like crystals and non-stoichiometric form, which are similar to those of bone apatite, can be obtained.

Acknowledgment

The authors thank PRA (Sino-France advanced research programme), NSF-C (No. 59872026) and the Postdoctoral Starting Fund of Xi'an Jiaotong University for subsidizing this study.

References

1. A. S. POSNER, *Physiol. Rev*. **49** (1969) 760.
2. J. S. HANKER and B. L. GLAMMARA, *Science* **242** (1988) 885.
3. G. L. DE LANGE and K. DONATH, *Biomaterials* **10** (1989) 121.
4. P. DUCHEYNE, J. CUCKLER, B. EVANS and S. RADIN, *ibid.* **11** (1990) 53.
5. P. DUCHEYNE, L. L. HENCH, A. KAGAN, M. MARTENS, A. BURSSENS and J. C. MULTER, *J. Biomed. Mater. Res.* **14** (1980) 225.
6. S. D. COOK, K. A. THOMAS, J. F. KAY and M. JARCHO, *Clin. Orthop. Rel. Res.* **232** (1988) 225.
7. P. DUCHEYNE and K. HEALY, *J. Biomed. Mater. Res.* **2** (1981) 137.
8. S. J. YANKEE and B. J. PLETKA, in ''Proceedings of the Third National Thermal Spray Conference'' (1990) p. 433.
9. P. E. WANG and T. K. CHAKI, *J. Mater. Sci. Mater. Med.* **6** (1995) 94.
10. C. Y. YANG, *ibid.* **6** (1995) 249.
11. L. G. ELLIES, D. G. A. NELSON and J. D. B. FEATHER, *Biomaterials* **13** (1992) 313.
12. R. M. BILTZ and E. D. PELLEGRINO, *J. Dent. Res.* **62** (1983) 1190.
13. A. TISELIUS, S. HJERTEN and O. LEVIN, *Arch. Biochem. Biophys.* **65** (1956) 132.
14. J. REDEPENNING and J. P. MCLSAAC, *Chem. Mater.* **2** (1990) 625.
15. M. SHIRKHANZADEH, *J. Mater. Sci. Lett.* **10** (1991) 1415.
16. *Idem., J. Mater. Sci. Mater. Med.* **6** (1995) 95.
17. J. REDEPENNING, T. SCHLESSINGER, S. BURNHAM, L. LIPPIELLO and J. MIYANO, *J. Biomed. Mater. Res.* **30** (1996) 287.
18. S. D. COOK, J. F. KAY, K. A. THOMAS and M. JARCHO, *Int. J. Oral Maxillofac. Impl.* **2** (1987) 15.
19. F. W. SHI, C. T. XIA, B. G. WANG and W. H. ZHONG, *J. Inorg. Mater.* **11** (1996) 193.

Received 20 May 1997
and accepted 4 March 1998